

01 Jan 2023

Experimental Study for Improving the Productivity of Laser Foil Printing

Tunay Turk

Ming-Chuan Leu

Missouri University of Science and Technology, mleu@mst.edu

Follow this and additional works at: https://scholarsmine.mst.edu/mec_aereng_facwork



Part of the [Aerospace Engineering Commons](#), and the [Mechanical Engineering Commons](#)

Recommended Citation

T. Turk and M. Leu, "Experimental Study for Improving the Productivity of Laser Foil Printing," *International Journal of Advanced Manufacturing Technology*, Springer, Jan 2023.

The definitive version is available at <https://doi.org/10.1007/s00170-023-11076-y>

This Article - Journal is brought to you for free and open access by Scholars' Mine. It has been accepted for inclusion in Mechanical and Aerospace Engineering Faculty Research & Creative Works by an authorized administrator of Scholars' Mine. This work is protected by U. S. Copyright Law. Unauthorized use including reproduction for redistribution requires the permission of the copyright holder. For more information, please contact scholarsmine@mst.edu.



Experimental study for improving the productivity of laser foil printing

Tunay Turk¹ · Ming C. Leu¹

Received: 11 November 2022 / Accepted: 6 February 2023
© The Author(s), under exclusive licence to Springer-Verlag London Ltd., part of Springer Nature 2023

Abstract

This study aims to improve the productivity of laser foil printing (LFP), which is a foil-based metal additive manufacturing (AM) process. LFP uses a dual-laser system to fabricate a 3-dimensional part in a layered fashion by performing four steps in each layer: spot welding, pattern welding, contour cutting, and edge polishing, all of which performed by use of lasers. We experimentally examined the welding and polishing steps in this study to enhance LFP productivity. The jump speed, dwelling duration, and weld path of spot welding and the line welding speed and wait time between weld lines of pattern welding are determined to minimize the LFP processing time, resulting in an eightfold increase in part fabrication productivity. Furthermore, we introduce laser edge polishing, vs. mechanical edge polishing done previously, to reduce the edge polishing time and further increase the productivity of the automated LFP process. For the laser polishing, we study laser polishing pattern (line- or spot-type polishing), polishing area, and overlapping ratio.

Keywords Metal additive manufacturing · Sheet lamination · Laser processing · Laser welding · Laser cutting · Laser polishing

1 Introduction

Laser foil printing (LFP) is a metal additive manufacturing (AM) process recently developed at the Missouri University of Science and Technology [1]. In this process, metal foils are the feedstock, and two different types of lasers perform part building and excess foil removal operations layer-by-layer. This metal AM method has been demonstrated to have a variety of potential application areas [2]. According to the American Society for Testing and Materials (ASTM) standard terminology for AM technologies, this method belongs to the AM category of sheet lamination [3, 4].

Our previous studies have shown that LFP has some distinct advantages over other metal AM methods. First, due to the higher thermal conductivity of foils over powders, LFP has a higher cooling rate and faster solidification when compared to powder-based metal AM techniques.

As a result, depending on the scanning direction, 10–15% higher strength for LFP parts was achieved compared to the laser powder bed fusion (LPBF) process, alongside finer grains in the material microstructure [5]. A high cooling rate is essential to form amorphous structures, also known as metallic glasses (MG) [6]. LFP has demonstrated its effectiveness in AM of zirconium-based MG ($Zr_{52.5}Ti_5Al_{10}Ni_{14.6}Cu_{17.9}$) sheets onto a bulk MG substrate [7], a Ti-6Al-4 V substrate [8], and other crystalline metal substrates [9] to form 3D bulk MG parts. Compression molding, injection molding, and die casting are different applications that can build metallic glass parts with thin sections without geometry flexibility [10], while LFP is an AM technique that can make 3-dimensional bulk MG parts with geometry flexibility. Second, the use of foil feedstock makes LFP easier to operate as no preheating and pre-processing is needed for the foil feed. On the other hand, powders are generally preprocessed by atomizing [11] and spheroidization [12, 13], and during the processing they need to be preheated [14] and well-spread on the powder bed [15]. In addition, during the material change, the LFP system does not need to be cleaned, making LFP a potential application area for additive manufacturing of multiple

✉ Tunay Turk
ttnpd@mst.edu

¹ Department of Mechanical and Aerospace Engineering,
Missouri University of Science and Technology, 400 W 13th
St, Rolla, MO 65409, USA

materials. In our previous studies of laser-foil-printing of bulk MGs, some intermediate layers were printed onto dissimilar material substrates in order not to contain brittle intermetallics [8, 9, 16].

Ultrasonic additive manufacturing (UAM) is another sheet lamination process that uses metal foils to build parts layer-by-layer. UAM is capable of building parts with layers of dissimilar materials and embedding functional components between layers [17]. LFP also has been shown to have the ability to fabricate parts with dissimilar materials [9], as well as to embed sensors [2]. The main advantages of LFP over UAM are as follows: (1) unlike UAM, LFP does not require using computer numerically controlled (CNC) milling operation to form the desired part shape that UAM needs, and (2) LFP fabricated parts have finer grains and higher strengths because of phase transformation of the part material [17].

LFP has been demonstrated for its ability to fabricate parts with various materials such as aluminum 1100 [18, 19], AISI 1010 low carbon steel alloy [2], 304L stainless steel [5, 20, 21], and Zr-based bulk MG [7–9], [16, 22, 23]. However, as a recently automated method [20], LFP needs to be more productive to find its place in the industry. Before the study described in the present paper, two different automation methods were investigated previously, changing the order of fabrication and incorporating laser polishing steps to increase productivity and decrease the risk of potential errors [24].

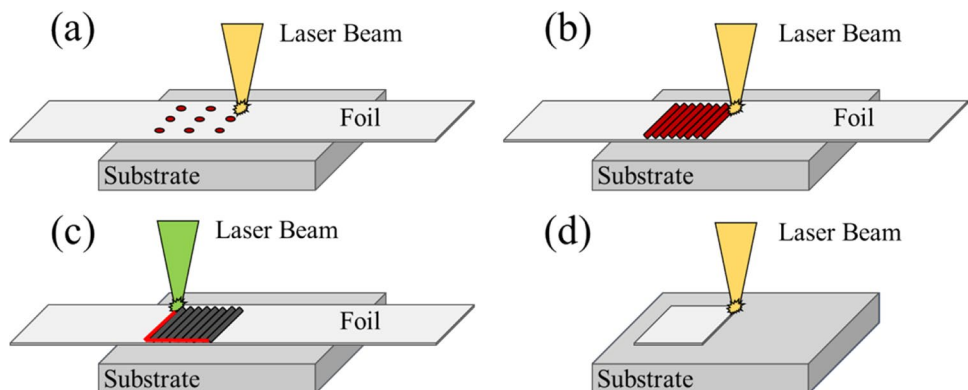
This study is aimed at improving the productivity of the LFP process significantly. In the present paper, first, the LFP process steps and system will be described and demonstrated. Then, the laser processing parameters for spot-welding and pattern-welding steps will be investigated and experimented. As a result of the experiments, the total time spent on welding in building of sample parts will be compared, and the optimal values of welding process parameters will be identified. Then, an experimental investigation will be conducted on laser edge polishing.

2 Laser foil printing process and system

Figure 1 illustrates the four main steps of the LFP process for the building of each part layer. The first step is laser spot welding. This step provides a temporary attachment of the fed foil to the previous layer in order not to have any thermal distortion during the next step, which is pattern welding. Laser spot welding is used as a temporary attachment because it has a faster cooling rate and, therefore, a rapid solidification rate of the melt pool compared to line welding [25]. Although it is not common to have laser spot welding in metal AM techniques as a part-building process step, the keyhole-mode spot welding of metal AM parts has been used as a joining technology [26] in aerospace applications. In addition, laser spot welding has been used in the automotive industry for over two decades [27]. Pattern welding is the second step, where the actual bonding (welding) between the supplied foil and the previous layer happens. Therefore, the total volumetric energy input (VEI) is much higher for laser pattern welding than for laser spot welding. After pattern welding, the next step is laser contour cutting to remove the excess foil to form the desired part geometry. The laser cutting causes edge elevation of the unwelded portion due to the power of the cutting operation. Hence, the last step is edge polishing to remove elevated edges to ensure that the surface is flat enough for the next layer to be printed on top. The edge polishing method used before this study was mechanical polishing [20]. Although mechanical polishing is effective in removing elevated edges, it is not a productive method as it takes a significant amount of time (10–15 min, depending on the size of the part geometry) and is prone to errors. In this study, we will introduce a laser polishing method based on some earlier research work [24].

Figure 2 shows the automated LFP system that has been developed and constructed in-house at Missouri S&T. This system consists of dual lasers for welding and cutting operations. The first laser is IPG YLP-1000, which is a continuous-wave (CW) infrared (IR) fiber laser with a maximum

Fig. 1 Illustration of process steps of the LFP: **a** spot welding, **b** pattern welding, **c** contour cutting, and **d** edge polishing



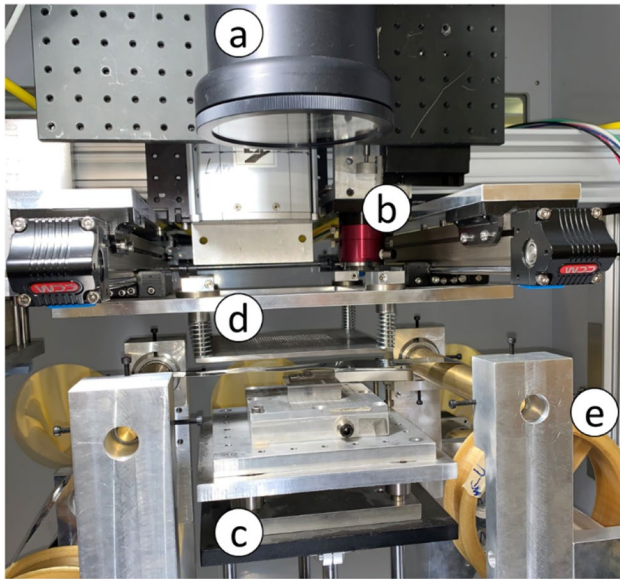


Fig. 2 Photo of the in-house developed automated LFP system. (a) Laser scanner, (b) laser cutting head, (c) gantry subsystem, (d) foil clamping plate, (e) roller-to-roller foil supply mechanism

power of 1000 W, a central wavelength of 1070 nm, a beam quality factor (M2) of 3.04, F-θ lens focal length of 330 mm, and laser spot size of 0.16 mm. This laser performs the spot welding and pattern welding steps, and a galvo-mirror scanner (SCANLAB hurrySCAN-30) is used to direct the laser beam to the desired location at any given time. The second laser is Coherent AVIA-355X, which is an ultraviolet (UV) pulsed laser with a maximum power of 10 W, pulse frequency of 100 kHz, and pulse duration of 30 ns. This laser performs the contour-cutting process step and has a laser cutting head with a focal length of 100 mm and a laser spot size of 0.04 mm. In addition to the dual lasers, the LFP system has a tri-axis (X, Y, Z) gantry subsystem to move the part around for the laser processing. Also, a foil clamping plate is used to move the foil back and forth to maintain its flatness during the spot-welding operation, and a roller-to-roller foil supply mechanism is used to feed the foil.

3 Laser welding

This section describes an experimental investigation for spot-welding and pattern-welding, both using the continuous-wave infrared fiber laser. Spot welding is applied before pattern welding to maintain the requirement of the fed foil not to be distorted during the pattern welding. A bi-directional line type of pattern welding is applied to the foil feed to bond the foil to the previous layer, as shown in Fig. 3. These two types of welding can be explained by using the volumetric energy input (VEI), which can be calculated with

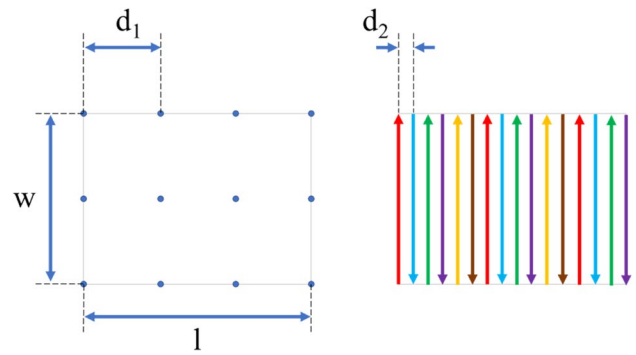


Fig. 3 Illustration of foil sample dimensions and distances between laser spots in spot welding and between laser lines in pattern welding

Eqs. (1) and (2) for line and spot types of welding, respectively [5, 28]:

$$VEI_{line} = \frac{P}{v \cdot h \cdot s} \tag{1}$$

$$VEI_{spot} = \frac{P \cdot t}{D_p \cdot h \cdot s} \tag{2}$$

In this study, the laser power (P) was 400 W, and the layer thickness (s) was 0.127 mm (0.005 in). The laser scanning speed (v), hatch space (h), point distance (D_p), and dwelling time (t) were varied.

During the experimental work to determine the optimum laser welding process parameters, 36-mm × 18-mm (1 × w as given in Fig. 3) rectangular samples were built and compared in terms of welding success and processing time. The feed material used is 304L stainless steel (SS) foil with a thickness of 0.127 mm purchased from Ulbrich Stainless Steels & Special Metals, Inc.

Before the present study, laser spot welding was applied with a clamping plate assembly (Fig. 2(d)) and the distance between two neighboring laser spots was set as 1 mm (distance d₁ in Fig. 3). As shown in Fig. 4, the

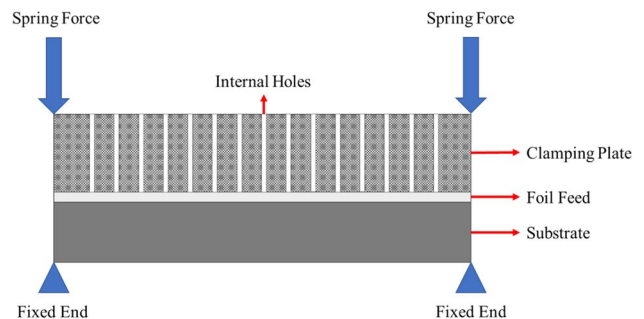


Fig. 4 Illustration of the clamping plate used to maintain the flatness of the fed foil

holed geometry of the clamping plate allows the laser spots to pass through. However, the holes in the clamping plate were 3 mm apart; therefore, nine different locations of the clamping plate were needed to provide a 1-mm spot distance. This entire spot-welding process took 8 min as given in Table 1. For pattern welding, line welding was applied with 8-s waiting time between two neighboring lines. The 8-s wait was required due to the high power of pattern welding, which could make the foil distorted and, as a result of the distortion, the foil burns and the line welding becomes unsuccessful. The 8-s wait time helps the line-welding process become more stable but requires a longer processing time (see in Table 1). In Fig. 3, the sample part geometry is designed to have $l=36$ mm and $d_2=0.1$ mm; there are 360 lines for the part, and 8 s of wait time for each line means 2880 s spent on waiting. With this approach, the wait time is very long, making the LFP a low-productivity process.

The abovementioned laser spot-welding and pattern-welding process steps have five different parameters that need to be determined and optimized in our experimental work as follows:

- Pattern welding parameters:

Parameter no. 1: Pattern line welding speed

Parameter no. 2: Wait time between pattern weld lines

- Spot welding parameters:

Parameter no. 3: Jump speed between two spots

Parameter no. 4: Dwelling duration at each spot

Parameter no. 5: Spot welding pattern

Fifteen different samples were fabricated using the LFP process with varying process parameters to find the optimum values of the above five parameters. The parameter values used, and the results of those samples are tabulated in Table 2.

3.1 Laser welding parameter no. 1: Pattern line welding speed

The first parameter affecting the feedstock material’s welding mode is the pattern line welding speed. The comparative results for the welding modes of LFP in an earlier study showed that the conduction mode should be preferred over the keyhole mode [21], because the conduction welding mode results in lower porosity (0.1% vs. 0.5%) and higher elongation rates in x -direction (69% vs. 61%) and z -direction (94% vs. 71%) [21].

Figure 5 shows the results of variable welding speeds. The aspect ratio (AR) is the ratio of depth (D) over width (W) of the weld pool, as given in Fig. 5. AR is used to determine if the welding mode is in conduction or keyhole mode. Generally, $AR < 1$ is accepted as the conduction-mode

Table 1 Process steps and time durations before the present study

General definition	Name/definition	Time
Spot welding	Spot welding with clamping plate	8 min
Pattern welding	Line welding	48 min 23 s
Edge polishing	Mechanical polishing	15 min
	Σ	1 h 11 min 23 s

Table 2 Laser welding sample parameters

Sample no	Parameter no					Result
	1	2	3	4	5	
1	300 mm/s	0.0 s	5 mm/s	0.3 ms	Linear	Unsuccessful
2	300 mm/s	0.0 s	5 mm/s	0.3 ms	Linear	Unsuccessful
3	300 mm/s	0.0 s	5 mm/s	0.3 ms	Linear	Unsuccessful
4	300 mm/s	0.2 s	5 mm/s	0.3 ms	Linear	Successful
5	300 mm/s	0.2 s	10 mm/s	0.3 ms	Linear	Successful
6	300 mm/s	0.2 s	50 mm/s	0.3 ms	Linear	Unsuccessful
7	300 mm/s	0.2 s	20 mm/s	0.3 ms	Linear	Unsuccessful
8	300 mm/s	0.2 s	15 mm/s	0.3 ms	Linear	Unsuccessful
9	300 mm/s	0.2 s	15 mm/s	0.25 ms	Linear	Unsuccessful
10	300 mm/s	0.2 s	15 mm/s	0.2 ms	Linear	Unsuccessful
11	300 mm/s	0.2 s	15 mm/s	0.3 ms	Contour	Unsuccessful
12	300 mm/s	0.2 s	10 mm/s	0.3 ms	Contour	Successful
13	300 mm/s	0.2 s	15 mm/s	0.4 ms	Linear	Unsuccessful
14	300 mm/s	0.2 s	10 mm/s	0.3 ms	Contour	Successful
15	300 mm/s	0.2 s	10 mm/s	0.3 ms	Contour	Successful

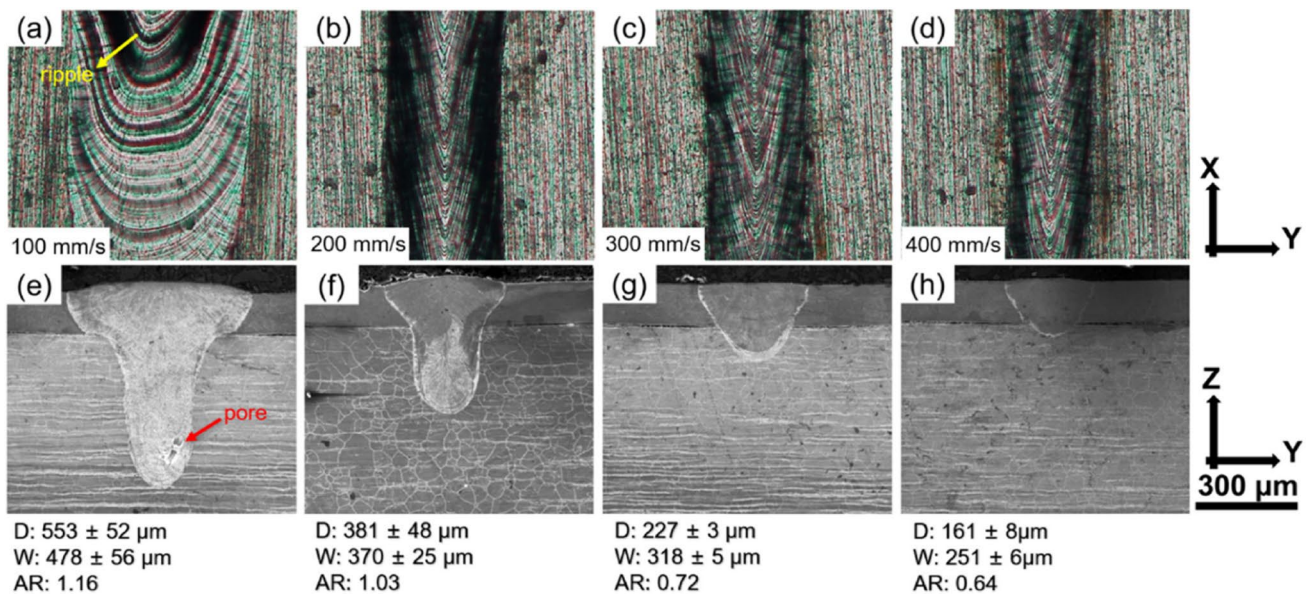


Fig. 5 Optical microscope (OM) images of single-track surface morphology (*X*–*Y* plane) at a laser power of 400 W and the scan speed of **a** 100 mm/s, **b** 200 mm/s, **c** 300 mm/s, and **d** 400 mm/s. The SEM

images of corresponding cross-section morphology (*Y*–*Z* plane) are shown in **(e–h)** [21]

welding [29]; thus, the results for 100 mm/s and 200 mm/s represent the keyhole-mode welding. Higher porosity in the keyhole-mode welding is due to the collapse of keyhole at the bottom of the keyhole [21]. As a result, keeping the laser power at 400 W and setting the line welding speed at 300 mm/s gave the best mechanical properties in the fabricated parts.

3.2 Laser welding parameter no. 2: Wait time between pattern weld lines

The second laser welding parameter is the wait time between pattern weld lines. We aim to minimize the wait time between weld lines. It is generally known that solidification of the melt pool helps avoid thermal distortion during line welding. Any instability in the melt pool may cause foil distortion, as shown in Fig. 6. Therefore, the melt pool needs to be solidified and cooled down to achieve a successful weld without burning the foil, and hence, waiting between weld lines is required in the process cycle.

However, melt pool solidification in pattern welding is not the only cause of foil distortion. Laser spot welding plays a vital role in foil stability. Before the present study, there were no additional spot-welding steps after applying the clamping plate on the foil, and the spacing between weld spots was physically limited to 1 mm with using the clamping plate. In the present study, we have developed one solution, as shown in Fig. 7, by applying additional spot welding, without use of any clamping plate, with a dense pattern of 0.25 mm in distance between two weld spots, in order to minimize the wait time between weld lines in pattern welding.

We have completed a set of experiments using the solution approach described above. As a result, the first three samples in Fig. 8 show some oxidation and burn; however, the fourth sample shows successful welding with a much more productive time. At the end of this set of experiments, the results show that no sample could be successfully fabricated without any wait time, but the wait time can be decreased significantly by an additional dense spot-welding step. The optimum laser welding parameter no. 2 is found to

Fig. 6 Illustration of **a** stable/flat surface after properly solidified melt pool, and **b** tilted/distorted surface after unstable melt pool

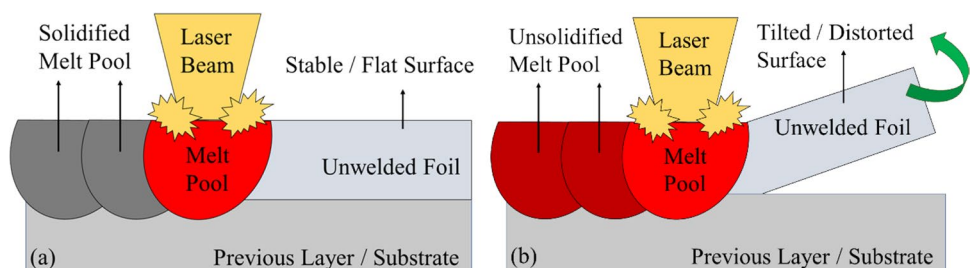


Fig. 7 Schematic of the suggested solution to determine the wait time between pattern weld lines

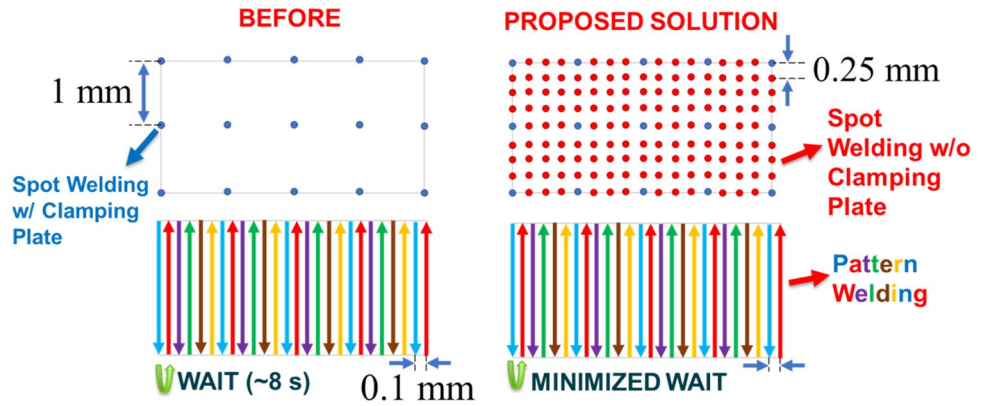


Fig. 8 Samples with varying wait times between weld lines. (All other parameters were set constant as follows: pattern line welding speed: 300 mm/s, jump speed of spot welding: 5 mm/s, dwelling duration of spot-welding: 0.3 ms, spot welding pattern: linear)

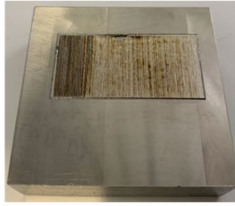
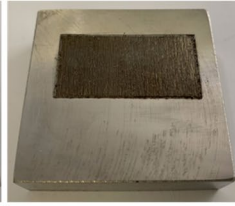
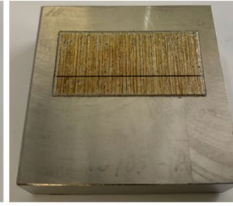
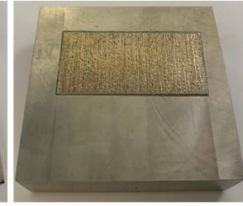
			
Sample #1	Sample #2	Sample #3	Sample #4
Wait Time: 0 s	Wait Time: 0 s	Wait Time: 0 s	Wait Time: 0.2 s
Result: Unsuccessful (Defects and burnt areas)	Result: Unsuccessful (Oxidation and burn)	Result: Unsuccessful (Burnt areas)	Result: Successful

Table 3 Pattern welding time comparison table with/without additional spot-welding step

	Before (8 s wait for each line):	After (0.2 s wait for each line):
Pattern welding time	23 s	23 s
Wait time between pattern weld lines	$360 \times 8 \text{ s} = 2880 \text{ s}$	$360 \times 0.2 \text{ s} = 72 \text{ s}$
Σ	48 min 23 s	1 min 35 s

be 0.2 s of wait time between two neighboring welding lines. Therefore, the time spent on pattern welding has reduced as given in Table 3. Note that in Table 3, the wait time is multiplied by the number of weld lines, i.e., 360. This is because the sample length is 36 mm, and the hatch space is 0.1 mm.

3.3 Laser welding parameter no. 3: Jump speed between two spots in spot welding

The third laser welding parameter is the jump speed between two neighboring spots in spot welding. This parameter was not considered before the present study because there was no spot-welding step without a foil clamping plate. Thus, there was no issue with foil distortion during the spot welding. However, after analyzing the comparative results in Table 3,

the significant productivity improvement shows that this new dense spot-welding step needs to be optimized.

Jump speed is the speed of the laser head when it moves between two weld spots. If the jump speed is too low, the LFP process will not be productive. If it is too high, then the melt pool of the weld spot will not be stable and, as a result, the spot welding will fail to provide a proper attachment of foil to the previous layer, as shown in Fig. 6. In other words, the foil is likely to be distorted if the melt pool of the spot weld does not solidify before the next spot weld and, as a result, welding will be unsuccessful.

Figure 9 shows the results of the experimental work. The change in jump speed resulted in successful welding for 5 mm/s and 10 mm/s. However, as the jump speed increases to 15 and 20 mm/s, the welding area is burnt, and the burnt area is larger for the higher speed. Thus, the jump speed should not exceed 10 mm/s.

3.4 Laser welding parameter no. 4: Dwelling duration at each spot in spot welding

The time spent at each spot, i.e., the dwelling duration, in spot welding is the fourth laser welding parameter. A larger time spent will result in a lower productivity and a higher VEI; however, a dwelling duration too low will result in foil detachment during the pattern welding. Therefore, this parameter should be optimized with use of experimental work.

Dwelling duration is a minor parameter in the LFP productivity analysis because its effect on productivity is relatively small. In the experiments, dwelling duration varied between 0.2 and 0.4 ms. For 0.2-ms dwelling duration, the total time spent on dwelling time for this sample is 2.1 s; for 0.4 ms, it is 4.2 s. To find out which duration works best, a comparative analysis is done for the burnt area among the unsuccessful samples. The samples with the jump speed of 15 mm/s are first analyzed according to their different dwelling durations. The first three samples in Fig. 10 show that the burnt area is larger at 0.2-ms dwelling duration and smaller at 0.3 ms, but the burnt area becomes larger at 0.4-ms dwelling duration because of some distortion at the sample's side end. Thus, the optimum value for dwelling duration is 0.3 ms for spot welding. Moreover, the 0.3-ms dwelling duration with the jump speed of 10 mm/s for the fourth sample in Fig. 10 resulted in successful pattern welding.

3.5 Laser welding parameter no. 5: Spot welding pattern

The fifth laser welding parameter is the spot-welding pattern. The experimented patterns included linear pattern and contour pattern, as shown in Fig. 11. This is not a critical parameter because the samples (samples no. 4 and no. 12 in Fig. 12) are successful for both patterns when the spot-welding jump speed is 10 mm/s. Figure 12 also shows that the results of both sample no. 8 and sample no. 11 are unsuccessful due to the high spot-welding jump speed of 15 mm/s; however, the burn area is much less for the contour pattern than the linear pattern. This is because continuous application of weld spots to one side of the foil will result in some foil distortion. Therefore, a better way to do spot welding is using the contour pattern, i.e., to begin the spot welding from a corner and follow the contour from the outer contour to the center.

Fig. 9 Samples with varying jump speeds of spot-welding. (All other parameters were set constant as follows: Pattern line welding speed: 0.3 m/s, wait time between pattern weld lines: 0.2 s, dwelling duration of spot-welding: 0.3 ms, spot welding pattern: linear)

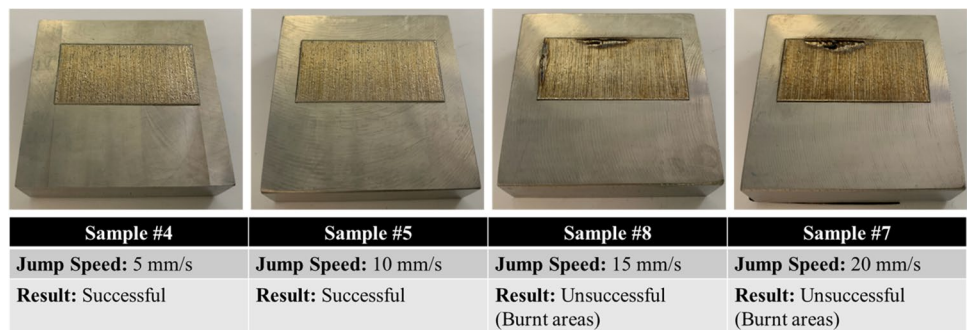


Fig. 10 Samples with varying dwelling durations of spot welding. (All other parameters were set constant as follows: pattern line welding speed: 0.3 m/s, wait time between pattern weld lines: 0.2 s, spot welding pattern: linear.)

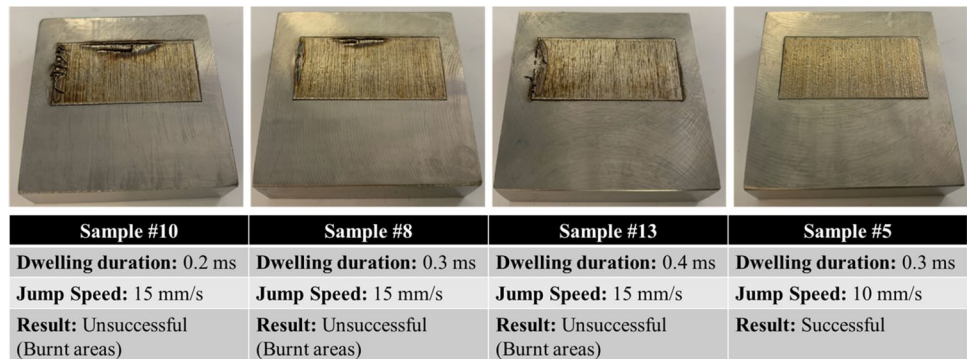


Fig. 11 Spot welding patterns: linear (left) and contour (right)

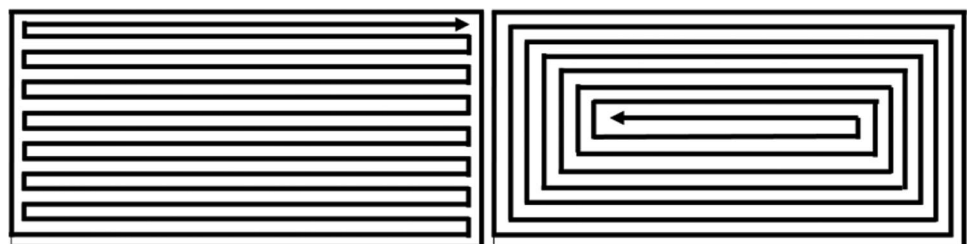
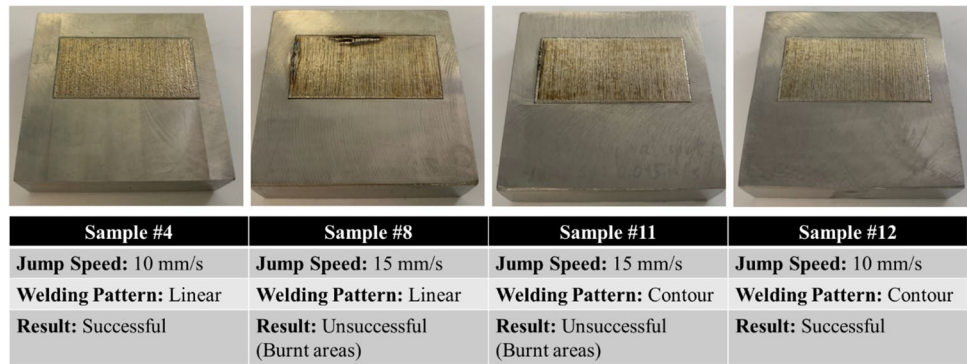


Fig. 12 Samples with varying spot-welding patterns. (All other parameters were set constant as follows: pattern line welding speed: 0.3 m/s, wait time between pattern weld lines: 0.2 s)



4 Edge polishing

Edge polishing is the last process step of a laser-foil-printed part. This step is essential as the next foil should lay on a flat surface. The previous study included mechanical polishing of the elevated edges [20], which was done by rubbing the edges back and forth against a stationary grindstone. Besides being slow, manual inspection was used to validate edges, making mechanical polishing prone to errors. Thus, a more efficient automated approach is needed to improve the LFP process productivity. Then, we proposed two alternative approaches to replace mechanical polishing. The first approach was to modify the order of fabrication steps, i.e., by exchanging the order of cutting and pattern welding in order not to have any raised edges. The second approach was to replace mechanical polishing with laser polishing. The first approach is faster as it does not involve any polishing step, but the second approach resulted in better accuracy with higher-quality parts [24]. Therefore, the present study focuses on laser polishing for reducing edge elevation to an acceptable level.

Laser polishing is an approach for surface quality improvement for additively manufactured metallic parts from materials such as steel, aluminum, cobalt-chromium, and titanium alloys [30]. The current CW fiber laser has been used by previous researchers to improve the surface quality of additive manufactured parts [31]. Also, the use of

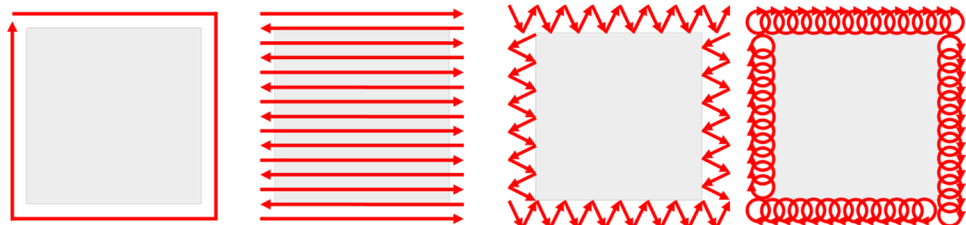
laser polishing to reduce the edge elevation of a part additively manufactured by the laser powder bed fusion (LPBF) process can be found in the literature [32].

In our experimental work of laser polishing, 30 square samples were LFP printed with a side length of 6 mm using the same foil feed used in the laser welding experiments. Figure 13 shows the different laser polishing patterns applied on the elevated edges. Regardless of the polishing pattern, laser polishing can be done by line polishing or spot polishing. Thus, the samples with polishing speeds in Fig. 14 are line polished, and the samples with dwelling durations are spot polished.

The polishing results are analyzed by surface scanning techniques. The scanning is done using the Gocator 2300 series laser surface profiler. The raw data output is post-processed by an in-house developed MATLAB program capable of creating of 3-dimensional surface plots and analysis of edge height. The average edge height (in Figs. 14, 15, and 18) is the average of 1000 highest edge points on a sample.

From Fig. 14, the spiral pattern using spot-type polishing gave the best results, which is due to the overlapping effect in the laser polishing. Additionally, to increase the accuracy of laser polishing, some different polishing widths have been experimented and the corresponding edge heights measured. The measured data of edge height vs. polishing width are shown in Fig. 15. The results show that the 0.1-mm width is insufficient as the edge height is significantly

Fig. 13 Illustration of laser polishing patterns (From left to right: linear edge pattern, all surface pattern, zigzag pattern, and spiral pattern)



larger than the others. The polishing widths of 0.2 mm and 0.3 mm width both cover all the elevated edge areas successfully. As a result, 0.3 mm is over-polishing as it gives no

better result than 0.2 mm in terms of edge height reduction. Thus, 0.2-mm width should be considered as the optimal polishing width.

Fig. 14 Edge height chart for various laser polishing parameter values [24]. The parameter values given in the horizontal axis have the unit of either mm/s for the laser scanning speed of line-type polishing, or μ s for the laser dwelling duration of spot-type polishing

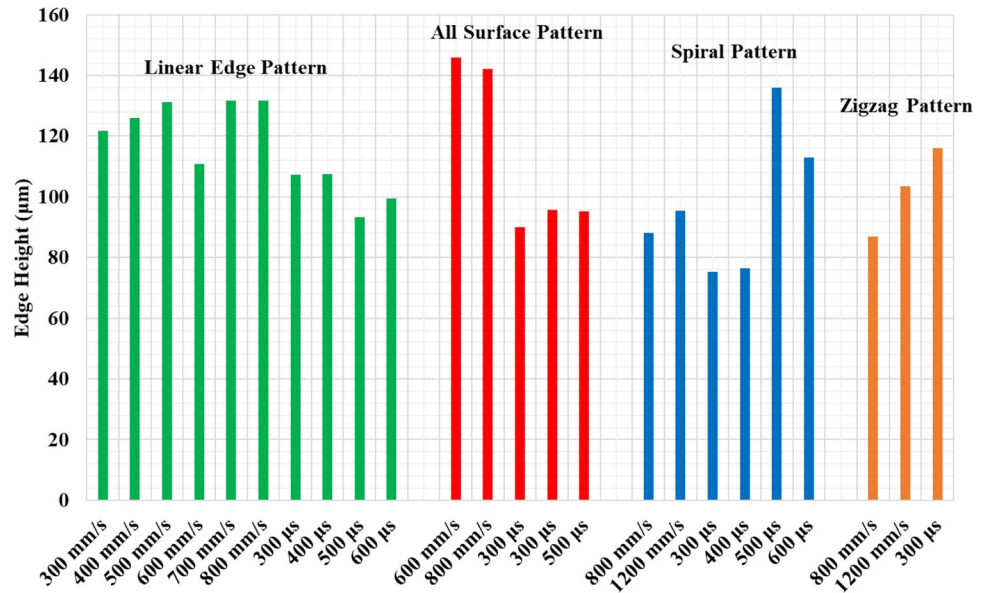


Fig. 15 Illustration of polishing width (left), and the measured edge height vs. polishing width (right)

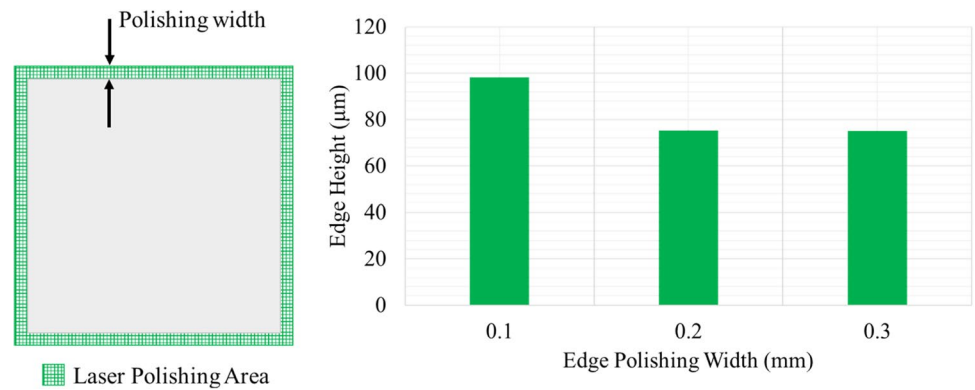
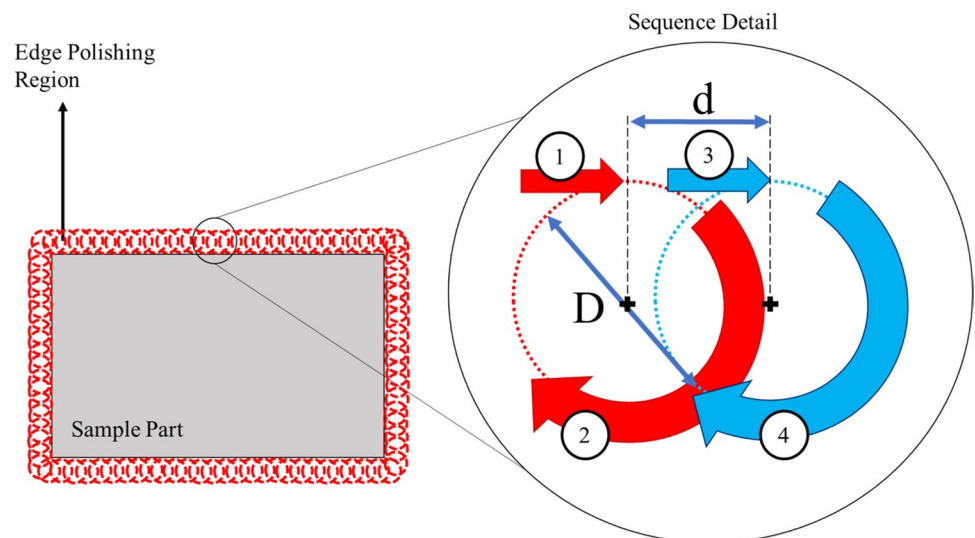


Fig. 16 Schematic illustration of spiral edge polishing pattern. (D diameter of the circle, d distance between the circles)



A schematic illustration of the spiral pattern is given in Fig. 16. The circle's diameter (D) used is the polishing width found above, which is 0.2 mm. Thus, the overlapping is affected by the distance (d) between two neighboring circles.

We did further experiments to investigate the overlapping effect, by finding its relationship with the laser beam spot size (D_1), which is 0.16 mm. Figure 17 demonstrates the area covered by laser spots with varying overlapping ratios. The ratio of laser beam spot size over the distance between circles is considered as the overlapping ratio (D_1/d). The distance between circles varied for low, medium, high, and very high overlapping ratios. All these are tabulated in Table 4 including the time spent on the edge polishing for the entire sample.

The results from the overlapping experiments are shown in Fig. 18. It shows the effectiveness of overlapping, and the edge's height dropped substantially for high overlapping. However, the very high overlapping shows little improvement compared to the high overlapping. Also, from Table 4, the time duration makes the very high overlapping unpractical.

Figure 19 shows the surface height of an LFP sample before and after polishing using the optimal width and high overlapping, with the data plotted using in-house developed MATLAB code.

Table 4 Overlapping ratios and time durations

Overlapping	D_1	d	D_1/d	Polishing duration
Low	0.16 mm	0.2 mm	0.8	26.2 s
Medium	0.16 mm	0.1 mm	1.6	41.6 s
High	0.16 mm	0.05 mm	3.2	74.7 s
Very high	0.16 mm	0.025 mm	6.4	138.1 s

5 Discussion

The VEI values of line- and spot-welding steps are calculated using Eqs. (1) and (2). For spiral-spot polishing, the dimensional parameters in Fig. 16 should be taken into consideration, which are the polishing width (D) and the distance between circles (d). Thus, the VEI calculation equations are given below as Eq. (3):

$$VEI_{\text{polishing-spiralspots}} = \frac{P \cdot t_c}{s \cdot D \cdot d} \quad (3)$$

In Table 5, line welding for 300 mm/s scanning speed shows the actual volumetric energy input for pattern welding. Thus, this VEI value of 104.98 J/mm³ can be used a reference value to

Fig. 17 Overlapping illustration for (i) low overlapping, (ii) medium overlapping, (iii) high overlapping, and (iv) very high overlapping. The top image shows the path for the spiral pattern, the bottom image shows the laser beams' overlapping for each spot of the spiral path

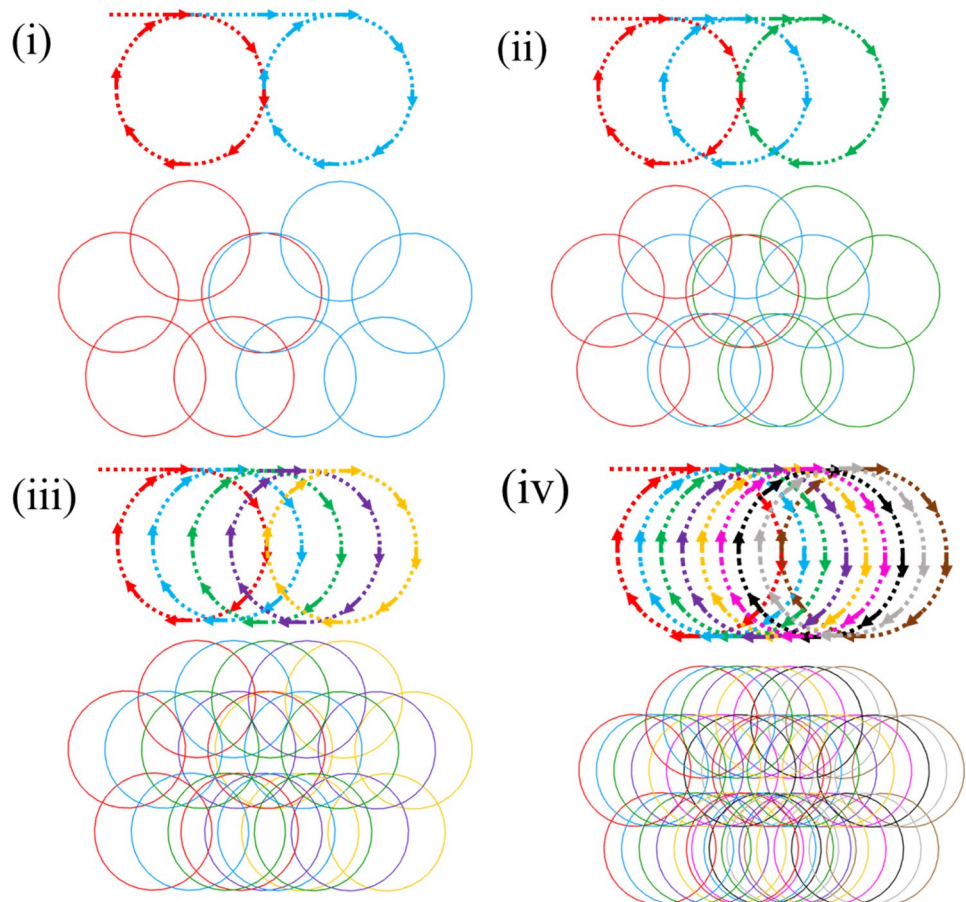


Fig. 18 Overlapping of spiral polishing vs. edge height

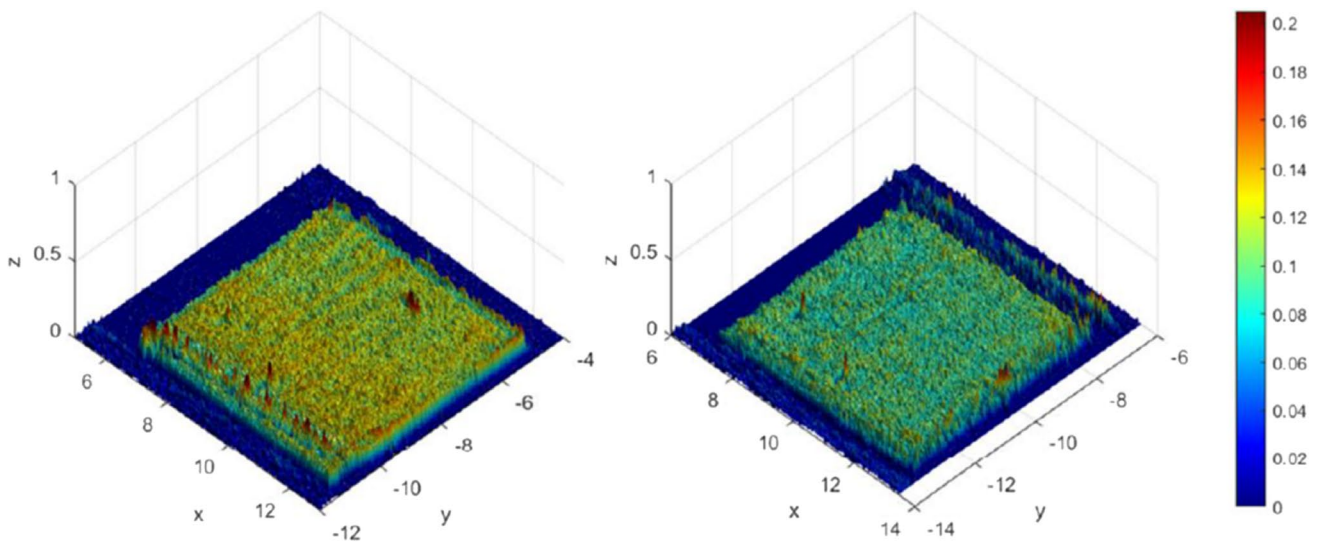
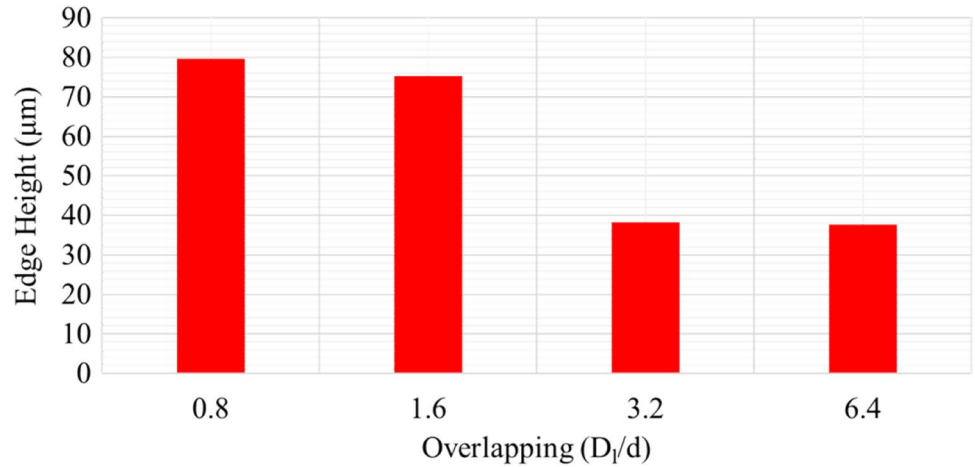


Fig. 19 MATLAB plots of LFP sample surface before and after laser polishing

Table 5 Laser line welding, spot welding, and spiral spot polishing volumetric energy input (P laser power, h hatch space, s layer thickness, v scanning speed, VEI volumetric energy input, t dwelling duration, t_c total dwelling duration in one circle, D_p point distance, D polishing width, d distance between circles)

	P	h	s	v	VEI
Line welding	400 W	0.1 mm	0.127 mm	300 mm/s	104.98 J/mm ³
Spot welding	400 W	0.3 ms	0.25 mm	0.25 mm	15.11 J/mm ³
Spot polishing	400 W	1.5 ms	0.127 mm	0.2 mm	118.11 J/mm ³
				0.1 mm	236.22 J/mm ³
				0.05 mm	472.44 J/mm ³
				0.025 mm	944.88 J/mm ³

explain the effectiveness of other operations, such as laser polishing and laser spot welding. It can be seen in Table 5 that the spot welding VEI is much lower than pattern welding because spot welding temporarily attaches the foil and ensures foil flatness during the pattern welding. On the other hand, the VEI

values for polishing need to be higher than pattern welding because polishing remelts and flattens the elevated edges to ensure a flat surface before the next layer of printing.

In this study, we have determined some processing parameters for laser foil printing that are highly important for LFP

process productivity. For 304L stainless steel, the optimal values are 300 mm/s line speed and 0.2-s wait time between weld lines for pattern welding, and 10 mm/s jump speed, 0.3 ms dwelling duration, and contour pattern for spot welding. With use of this optimal set of laser welding parameters, the total welding time is reduced from 56 min 23 s before this study to 7 min 12 s after this study, which is an 87.1% time reduction, as given in Table 6. Importantly, an additional dense-spot welding step (indicated in Table 6 as spot welding without plate) plays a vital role in this timesaving. This step uses no clamping plate application on the top of the foil. As a result, the wait time between the lines in pattern welding is greatly reduced.

In addition to the laser welding study, a laser edge polishing study has been conducted. In the edge polishing study, the effects of laser polishing pattern, area of application, and overlapping ratio were determined, and a comparative study was completed to determine the best laser polishing pattern. Among the four different patterns of linear edge, all-surface, zigzag, and spiral, the spiral pattern was determined as the most effective laser polishing pattern. The more overlapping showed better results until $D/d=3.2$, after that the overlapping had no improvement in lowering raised edges. In addition, spot-type laser polishing was found to be more effective than line-type laser polishing. The rationale is that laser spot polishing not only remelts but also causes erosion to the raised edges. Laser erosion in the literature of selective laser erosion (SLE) is caused by laser ablation with high energy and short time duration [33]. Although SLE application in the literature uses a different type of laser (Nd:YAG laser), different process parameters, and material type

(AISI 1045 steel), the results showed that the spot application's edge elevation reduction is more effective than line-type laser polishing. The microsecond spot laser application created a shock wave and resulted in remelting and erosion to effectively remove raised edges. Furthermore, only remelting causes bulge formation in line polishing without laser erosion, and the results are unsatisfactory. The remelted portion of the edges will still be above the surface level. Figure 20 shows the optical microscope (OM) images for the top left corner of laser polishing samples to visualize the surface texture difference in spot-type vs. line-type of edge polishing.

This study has shown that the automated method of laser polishing could be integrated into the LFP part-building parameters, and this also helps the process to reduce time spent on the entire edge suppression. Before the laser polishing application, mechanical polishing took around 15 min. After this study, laser polishing can reliably remove elevated edges in much less time, from 15 min to just 74.7 s, which is around 91.7% of time reduction. Table 6 includes the results of edge polishing before and after this study, for each of the LFP steps except the contour-cutting step. It shows that this study results in 88.1% in time reduction for the total laser welding and polishing time.

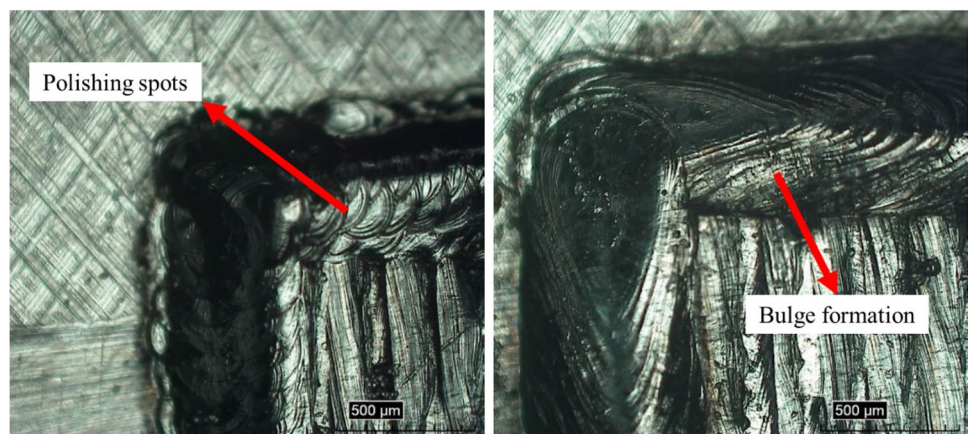
6 Conclusion

This paper investigated automating the laser foil printing process, which consists of spot welding, pattern welding, and edge polishing, all by using lasers, in the fabrication of each layer. The

Table 6 Process steps — time durations for LFP steps before/after this study

General definition	Step no	Name/definition	Time before this study	Time after this study
Spot welding	1	Spot welding with plate	8 min	1 min
	2	Spot welding without plate	N/A	4 min 37 s
Pattern welding	3	Line welding	48 min 23 s	1 min 35 s
Edge polishing	4	Mechanical or laser polishing	15 min	1 min 15 s
		Σ	1 h 11 min 23 s	8 min 27 s

Fig. 20 Optical microscope images for showing the surface texture of spiral pattern laser polishing with spots (left), and line scanning (right)



results showed an 88.1% reduction in processing duration for laser spot-welding, pattern-welding, and edge polishing. Among the LFP processing steps, laser spot welding is a crucial step to ensure faster welding. Therefore, an additional spot-welding step without a clamping plate is added to the LFP process cycle to greatly reduce the time spent waiting between weld lines in pattern welding. The rationale is that the denser spots help to provide a flat surface (by preventing the detachment of weld spots and thermal distortion of the fed foil) during the high-energy, high-speed pattern welding. After this study, among the investigated process steps, the most time is spent on laser spot welding because the most challenging issue in the LFP process is the flatness of foil during the laser pattern welding. Another major improvement in the LFP process is laser polishing, which enables an automated way of eliminating the edge elevation with the current equipment. The overlapping effect of the spiral pattern with laser spots resulted in a faster approach and better-quality edges. Spot-type laser polishing caused a combination of laser melting and erosion, resulting in the lowest edge height among all alternative laser polishing methods.

Author contribution Conceptualization: Tunay Turk.
Methodology: Tunay Turk.
Formal analysis: Tunay Turk.
Investigation: Tunay Turk, Ming C. Leu.
Supervision: Ming C. Leu.
Funding acquisition: Ming C. Leu.
Writing — original draft: Tunay Turk.
Writing — review and editing: Tunay Turk, Ming C. Leu.

Funding This research was funded by the Intelligent Systems Center at the Missouri University of Science and Technology.

Data availability The raw/processed data required to reproduce these findings will be available on email request.

Code availability Not applicable.

Declarations

Ethics approval The manuscript contains original ideas which have never been published before in other journals.

Consent to participate This study is not a human transplantation study. No consent needed for this paper.

Consent for publication The authors declare their consent for publication.

Competing interests The authors declare no competing interests.

References

1. Tsai H-L, Shen Y, Li Y, Chen C (2020) Foil-based additive manufacturing system and method. <https://www.osti.gov/biblio/1771599>. Accessed 10 Feb 2023
2. Chen C, Shen Y, Tsai H-L (2016) A foil-based additive manufacturing technology for metal parts. *J Manuf Sci Eng* 139(2). <https://doi.org/10.1115/1.4034139>
3. ISO/ASTM (2015) ISO/ASTM 52900: additive manufacturing - general principles - terminology. *Int Standard* 5:1–26. <https://www.iso.org/standard/69669.html>. Accessed 10 Feb 2023
4. Guo N, Leu MC (2013) Additive manufacturing: technology, applications and research needs. *Front Mech Eng* 8(3):215–243. <https://doi.org/10.1007/s11465-013-0248-8>
5. Hung C-H, Sutton A, Li Y, Shen Y, Tsai H-L, Leu MC (2019) Enhanced mechanical properties for 304L stainless steel parts fabricated by laser-foil-printing additive manufacturing. *J Manuf Process* 45:438–446. <https://doi.org/10.1016/j.jmapro.2019.07.030>
6. Wang WH, Dong C, Shek CH (2004) Bulk metallic glasses. *Mater Sci Eng R Rep* 44(2–3):45–89. <https://doi.org/10.1016/j.mser.2004.03.001>
7. Shen Y, Li Y, Chen C, Tsai H-L (2017) 3D printing of large, complex metallic glass structures. *Mater Des* 117:213–222. <https://doi.org/10.1016/j.matdes.2016.12.087>
8. Li Y, Shen Y, Leu MC, Tsai H-L (2018) Building Zr-based metallic glass part on Ti-6Al-4V substrate by laser-foil-printing additive manufacturing. *Acta Mater* 144:810–821. <https://doi.org/10.1016/j.actamat.2017.11.046>
9. Li Y, Shen Y, Chen C, Leu MC, Tsai H-L (2017) Building metallic glass structures on crystalline metal substrates by laser-foil-printing additive manufacturing. *J Mater Process Technol* 248:249–261. <https://doi.org/10.1016/j.jmatprotec.2017.05.032>
10. Schroers J (2010) Processing of bulk metallic glass. *Adv Mater* 22(14):1566–1597. <https://doi.org/10.1002/adma.200902776>
11. Sehhat MH, Sutton AT, Hung C-H, Newkirk JW, Leu MC (2022) Investigation of mechanical properties of parts fabricated with gas- and water-atomized 304L stainless steel powder in the laser powder bed fusion process. *JOM* 74(3):1088–1095. <https://doi.org/10.1007/s11837-021-05029-7>
12. Sehhat MH et al (2022) Plasma spheroidization of gas-atomized 304L stainless steel powder for laser powder bed fusion process. *Mater Sci Addit Manuf* 1(1):1. <https://doi.org/10.18063/msam.v1i1.1>
13. Sehhat MH, Chandler J, Yates Z (2022) A review on ICP powder plasma spheroidization process parameters. *Int J Refract Metals Hard Mater* 103:105764. <https://doi.org/10.1016/j.ijrmhm.2021.105764>
14. Liu T et al (2022) In-situ infrared thermographic inspection for local powder layer thickness measurement in laser powder bed fusion. *Addit Manuf* 55:102873. <https://doi.org/10.1016/j.addma.2022.102873>
15. Sehhat MH, Mahdianikhotbesara A (2021) Powder spreading in laser-powder bed fusion process. *Granul Matter* 23(4):89. <https://doi.org/10.1007/s10035-021-01162-x>
16. Li Y, Shen Y, Hung C-H, Leu MC, Tsai H-L (2018) Additive manufacturing of Zr-based metallic glass structures on 304 stainless steel substrates via V/Ti/Zr intermediate layers. *Mater Sci Eng, A* 729:185–195. <https://doi.org/10.1016/j.msea.2018.05.052>
17. Friel RJ, Harris RA (2013) Ultrasonic additive manufacturing – a hybrid production process for novel functional products. *Procedia CIRP* 6:35–40. <https://doi.org/10.1016/j.procir.2013.03.004>
18. Hung C-H et al (2020) Aluminum parts fabricated by laser-foil-printing additive manufacturing: processing, microstructure and mechanical properties. *Materials* 13(2). <https://doi.org/10.3390/ma13020414>
19. Sehhat MH, Behdani B, Hung C-H, Mahdianikhotbesara A (2021) Development of an empirical model on melt pool variation in laser foil printing additive manufacturing process using statistical

- analysis. *Metallogr, Microst, Anal* 10(5):684–691. <https://doi.org/10.1007/s13632-021-00795-x>
20. Hung C-H, Turk T, Sehhat MH, Leu MC (2022) Development and experimental study of an automated laser-foil-printing additive manufacturing system. *Rapid Prototyp J* 28(6):1013–1022. <https://doi.org/10.1108/RPJ-10-2021-0269>
 21. Hung C-H, Chen W-T, Sehhat MH, Leu MC (2021) The effect of laser welding modes on mechanical properties and microstructure of 304L stainless steel parts fabricated by laser-foil-printing additive manufacturing. *Int J Adv Manuf Technol* 112(3):867–877. <https://doi.org/10.1007/s00170-020-06402-7>
 22. Bordeenithikasem P, Shen Y, Tsai H-L, Hofmann DC (2018) Enhanced mechanical properties of additively manufactured bulk metallic glasses produced through laser foil printing from continuous sheetmetal feedstock. *Addit Manuf* 19:95–103. <https://doi.org/10.1016/j.addma.2017.11.010>
 23. Li Y, Shen Y, Leu MC, Tsai H-L (2019) Mechanical properties of Zr-based bulk metallic glass parts fabricated by laser-foil-printing additive manufacturing. *Mater Sci Eng, A* 743:404–411. <https://doi.org/10.1016/j.msea.2018.11.056>
 24. Turk T, Hung C-H, Sehhat MH, Leu MC (2021) Methods of automating the laser-foil-printing additive manufacturing process. In 2021 *Int Solid Freeform Fabr Symp* 1142–1153. Accessed: Jun. 05, 2022. [Online]. <https://repositories.lib.utexas.edu/handle/2152/90714>
 25. He X, Fuerschbach PW, DebRoy T (2003) Heat transfer and fluid flow during laser spot welding of 304 stainless steel. *J Phys D Appl Phys* 36(12):1388–1398. <https://doi.org/10.1088/0022-3727/36/12/306>
 26. Wits WW, Becker JMJ (2015) Laser beam welding of titanium additive manufactured parts. *Procedia CIRP* 28:70–75. <https://doi.org/10.1016/j.procir.2015.04.013>
 27. Yang YS, Lee SH (1999) A study on the joining strength of laser spot welding for automotive applications. *J Mater Process Technol* 94(2):151–156. [https://doi.org/10.1016/S0924-0136\(99\)00094-1](https://doi.org/10.1016/S0924-0136(99)00094-1)
 28. Fayazfar H et al (2018) A critical review of powder-based additive manufacturing of ferrous alloys: process parameters, microstructure and mechanical properties. *Mater Des* 144:98–128. <https://doi.org/10.1016/j.matdes.2018.02.018>
 29. Sibillano T, Ancona A, Berardi V, Schingaro E, Basile G, Lugarà PM (2007) Optical detection of conduction/keyhole mode transition in laser welding. *J Mater Process Technol* 191(1):364–367. <https://doi.org/10.1016/j.jmatprotec.2007.03.075>
 30. Basha SM, Bhuyan M, Basha MM, Venkaiah N, Sankar MR (2020) Laser polishing of 3D printed metallic components: a review on surface integrity. *Mater Today Proc* 26:2047–2054. <https://doi.org/10.1016/j.matpr.2020.02.443>
 31. Chen C, Tsai H-L (2018) Fundamental study of the bulge structure generated in laser polishing process. *Opt Lasers Eng* 107:54–61. <https://doi.org/10.1016/j.optlaseng.2018.03.006>
 32. Metelkova J, de Formanoir C, Haitjema H, Witvrouw A, Pflieger W, Hooreweder B (2019) Elevated edges of metal parts produced by laser powder bed fusion: characterization and post-process correction, in Joint Special Interest Group meeting between euspen and ASPE Advancing Precision in Additive Manufacturing, Date: 2019/09/16 - 2019/09/18, Location: Nantes, France. Accessed: Nov. 02, 2022. [Online]. <https://lirias.kuleuven.be/2905248?limo=0>
 33. Yasa E, Kruth J-P (2010) Investigation of laser and process parameters for selective laser erosion. *Precis Eng* 34(1):101–112. <https://doi.org/10.1016/j.precisioneng.2009.04.001>

Publisher's note Springer Nature remains neutral with regard to jurisdictional claims in published maps and institutional affiliations.

Springer Nature or its licensor (e.g. a society or other partner) holds exclusive rights to this article under a publishing agreement with the author(s) or other rightsholder(s); author self-archiving of the accepted manuscript version of this article is solely governed by the terms of such publishing agreement and applicable law.